Review of High Pressure Studies on Doped Bi_2Se_3 Superconductors

Takashi NAKA[1, *] Anne DE VISSER[2]

We present a review of the superconducting properties of Cu, Sr and Nb doped Bi_2Se_3 compounds with a focus on high pressure effects. The parent compound Bi_2Se_3 is a topological insulator at ambient pressure and exhibits pressure-induced crystallographic phase transitions and superconductivity above 10 GPa. The doped compounds are all bulk superconductors with $T_c \sim 3$ K and have been investigated intensively in the past decade because of their candidature for topological superconductivity (TSC). A key role as regards topological superconductivity is played by spontaneous rotational symmetry breaking (RSB), which is observed, for instance, as an anisotropy in the upper critical field B_{c2}. We discuss the pressure variation of T_c and the concomitant effect on the upper critical field. An analysis of the basal-plane anisotropy of B_{c2} is presented in the context of an odd-parity unconventional superconducting state.
[*topological superconductor, rotational symmetry breaking, resistivity, upper critical field, critical pressure*]

1. Introduction

Doped Bi_2Se_3 superconductors, with an optimum superconducting transition temperature T_c around 3 K, were realized by intercalation of metallic ions, such as Cu^+, Sr^{2+} and Nb^{2+}, into the three-dimensional topological insulator Bi_2Se_3 [1–4]. The parent compound Bi_2Se_3 is a prototypical topological insulator [5]: the bulk being an insulator, while the surface is conducting with linearly dispersing electron states (Dirac-cone) at the Fermi level, as demonstrated by angle-resolved photoemission spectroscopy (ARPES) measurements [6]. The surface states are protected by the nontrivial topological nature inherent to the bulk band structure. Even after carrier doping topological surface states are maintained in $Cu_xBi_2Se_3$ [6] in $Sr_xBi_2Se_3$ [7]. Doped Bi_2Se_3 is a candidate for realizing a topological superconducting (TSC) state, which is predicted to be unconventional with a time-reversal-invariant topological symmetry. Such a 3-dimensional topological superconductor has a full superconducting energy gap in the bulk and gapless Andreev bound states on its surface [8]. Therefore, TSCs are expected to be unique platforms for new quantum phenomena, related closely to those of unconventional superconductors, such as Sr_2RuO_4 and UPt_3 [9]. At the same time not only Bi_2Se_3 [10–13], but also Bi_2Te_3 [14,15] and Sb_2Se_3 [16] have been investigated in terms of an electronic topological transition (ETT) or Lifshitz transition. Such a transition was originally proposed theoretically by Lifshitz in 1960 when considering high pressure induced phenomena in metals at $T = 0$ [17]. It is related to a change of the Fermi surface topology of a metal induced by the application of pressure. Recently, Volovik categorized systematically ''topological Lifshitz transitions'' which are accompanied by a change of the topological invariance [18], which distinguishes these from conventional Lifshitz transition [13].

[1] National Institute for Materials Science, 1-2-1 Sengen, Tsukuba, Ibaraki 305-0047

[2] Van der Waals-Zeeman Institute, University of Amsterdam, Science Park 904, 1098 XH Amsterdam, The Netherlands

* Electronic address: naka.takashi@nims.go.jp

In this review, after reporting briefly the superconducting (SC) properties of $M_xBi_2Se_3$ (M = Cu, Sr and Nb) and their pressure dependencies [19–23], we focus on the recent high pressure studies of superconductivity in $Cu_{0.3}Bi_2Se_3$ and $Sr_{0.15}Bi_2Se_3$. For the latter it is shown that rotational symmetry breaking (RSB) is realized in the superconducting state upon the application of a magnetic field. Furthermore, RSB is strengthened under pressure. The RSBs for M = Cu and Sr reported recently [24–27] are reexamined and we speculate there is a scaling of the anisotropy of the upper critical field B_{c2}, a characteristic of the RSB, with respect to a critical pressure p_c where the superconductivity is suppressed. The anomalous divergence of the basal-plane anisotropy of B_{c2} at p_c provides a strong motivation to conduct a further investigation to reveal the driving force of the RSB appearing below the SC transition.

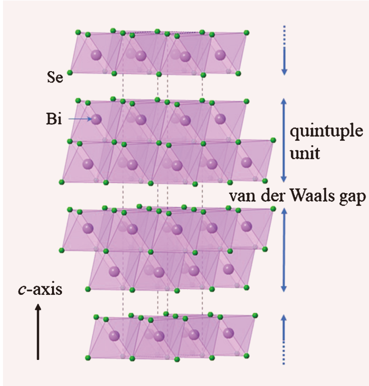

Fig. 1. (Color online) Crystallographic structure model of Bi_2Se_3 (space group: R-$3m$) determined at ambient pressure. The unit cell is visualized by dashed lines. The dopant ions, such as Cu^+, Sr^{2+} and Nb^{2+} are intercalated into the van der Waals gap established between the Bi_2Se_3 quintuple units stacked along the c-axis.

2. High pressure-induced phenomena in Bi_2Se_3 and Bi_2Se_3-based superconductors

The parent compound Bi_2Se_3 has a layered trigonal structure consisting of quintuple units (a block of 5 layers) stacked along the c-axis and hold together by the weak van der Waals bonding between the top and bottom Se layers of the units (Fig. 1). Dopant metallic ions, such as Cu^+, Sr^{2+} and Nb^{2+} can be intercalated into the van der Waals gap between the Bi_2Se_3 quintuple units and provide charge carriers [9]. In the case of M = Cu, which is the most intensively investigated material in the series, superconductivity emerges in the range $0.1 < x < 0.6$ with a Hall carrier concentration $n \approx 10^{19}$–10^{20} cm^{-3} [1]. As shown recently [19–23], the pressure-variation of T_c, dT_c/dp, in the $M_xBi_2Se_3$ series is negative for M = Cu and Sr, but positive for M = Nb (Table 1). According to the Hall carrier number $n(p)$ and resistivity $\rho(T, p)$ obtained for M = Cu and Sr, n and T_c decrease simultaneously with increasing pressure and a superconductor-to-semiconductor (or semimetal) transition is expected to occur at a critical pressure (p_c). The latter can be estimated by the extrapolation of the $T_c(p)$ curves to $T_c = 0$ [19–22]. It is noteworthy that for

Table 1. Superconducting parameters for the rhombohedral $M_xBi_2Se_3$ (M = Cu, Sr and Nb).

M	x	T_c(K)	l(nm)	ξ_a(nm)	ξ_{a^*}(nm)	ξ_c(nm)	γ^{aa^*}※	p_c(GPa)	dT_c/dp*	Ref.
Cu	0.30	3.5	34	13	—	4	—	6.3	N	[19]
	0.30	3.6	—	—	—	—	1.5	—	—	[26]
Sr	0.065	~3	—	—	—	—	—	~1.2	N	[20]
	0.10	2.8	—	—	—	—	6.8	—	—	[25]
	0.10	2.6	—	—	—	—	—	1.9	N	[21]
	0.15	3.0	—	19.6	7.6	5.4	3.2	3.5	N	[22,25]
Nb	0.25	3.4	50	19	—	9.5	—	—	P	[23]

※ $\gamma^{aa^*} = B^a_{c2}/B^{a^*}_{c2}$ measured at $p = 0$, * N and P represent dT_c/dp < 0 and > 0, respectively.

$Sr_xBi_2Se_3$ $p_c(x)$ increases with the dopant concentration x, while T_c at ambient pressure is nearly constant with respect to x (Table 1).

At high pressures above 3 GPa, $Sr_{0.065}Bi_2Se_3$ exhibits a sequence of crystallographic transitions: from the rhombohedral (R-3m) structure to monoclinic ($C2/m$) at p = 6 GPa and then to a body-centered tetragonal ($I4/mmm$) structure at 25 GPa [20]. Concomitantly, the resistivity $\rho(T)$ recovers to a metallic temperature variation and superconductivity reemerges at p∼6 GPa. The transition temperature $T_c(p)$ makes a steep increase to T_c = 8 K at p = 6 GPa and levels off to a value T_c = 7 K at 80 GPa. These pressure-induced crystallographic transitions and the reemergence of superconductivity for $Sr_{0.065}Bi_2Se_3$ are qualitatively similar to those reported for the parent compound Bi_2Se_3. In fact, Bi_2Se_3 exhibits crystallographic transitions from rhombohedral (R-3m) to monoclinic ($C2/m$) at 10 GPa, and then to a body-centered cubic-like structure ($C2/m$) at 28 GPa [10,12]. A pressure-induced superconducting transition occurs at a pressure slightly above 10 GPa. $T_c(p)$ increases steeply to 7 K at 28 GPa and then keeps a constant value up to 50 GPa [11]. Remarkably, even at pressures well below the structural transitions, crystallographic anomalies are found in Bi_2Se_3 [10] and also in isostructural Bi_2Te_3 [14] and Sb_2Se_3 [16]. For Bi_2Se_3 the lattice constant ratio c/a displays a minimum and the in-plane compressibility exhibits a kink at around 5 GPa [10], while these features are not revealed by the volume and lattice constants as a function of pressure. These pressure-induced phenomena can possibly be attributed to a Lifshitz transition or electron topological transition (ETT) [17], involving a change in the topology of the Fermi surface and, consequently, in the density of state at the Fermi level. Therefore, as discussed below, one needs to take into account crystallographic instabilities, especially, in the ab-plane as observed in Bi_2Se_3 [10] and Sb_2Se_3 [16].

3. Superconductivity under high pressure in $Cu_xBi_2Se_3$

The basic electronic properties of $Cu_{0.3}Bi_2Se_3$ have been determined by macroscopic measurements of the resistivity, specific heat, susceptibility and Hall effect [1,19]. These measurements show that the topological insulator Bi_2Se_3 can be turned into a bulk superconductor by intercalation of Cu. For several single crystals with x = 0.3 a bulk superconducting transition with an onset transition temperature T_c = 3.1 K is confirmed by resistivity and ac-susceptibility measurements [19]. At ambient pressure, the upper critical fields $B_{c2}{}^{ab}$ and $B_{c2}{}^{c}$, for a field applied in the ab-plane and along the c-axis, respectively, are estimated to be 5.6 and 1.9 T at T = 0 (see Fig. 2). Correspondingly, the in-plane coherence lengths ξ_{ab} is 13 nm and the out-of-plane coherence length ξ_c is 4 nm. Using the Hall carrier concentration n = 1.2×10^{26} m^{-3} and the residual resistivity ρ_0 = 1.5×10^{-6} Ωm [19], the electron mean free path l is estimated to be l = 34 nm, which shows that the superconductivity for the sample examined in Ref. [19] is in the clean limit $l>\xi$ and possibly could be unconventional, *i.e.* of the odd-parity type.

Based on the two-orbital model developed by Fu and Berg [8], the SC paring symmetry was derived for $Cu_xBi_2Se_3$ in the trigonal structure (crystal point group D_{3d}). For the D_{3d} point group four different pairing potentials Δ_1, Δ_2, Δ_3 and Δ_4 are obtained, with corresponding irreducible representations A_{1g}, A_{1u}, A_{2u} and E_u, respectively (see Fig. 3). Among these

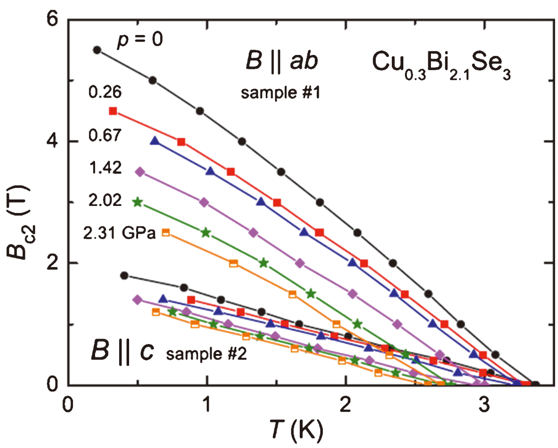

Fig. 2. (Color online) The temperature dependence of B_{c2} for $B//ab$-plane (upper six curves) and $B//c$-axis (lower six curves) at various pressures for $Cu_{0.3}Bi_2Se_3$ [19].

potentials only $\Delta_2(A_{1u})$ and $\Delta_4(E_u)$ have both a full SC gap and odd-parity symmetry [8,28]. After the discovery of RSB in $Cu_{0.3}Bi_2Se_3$ by nuclear magnetic resonance (NMR) measurements [24], Fu predicted that for the E_u representation the spin-orbit interaction associated with hexagonal warping makes the superconducting state fully gapped, giving rise to topological superconductivity [28]. Actually, as argued below, odd-parity pairing in the E_u representation of the D_{3d} crystal point group naturally breaks the rotational symmetry of the trigonal doped Bi_2Se_3.

Under hydrostatic pressure SC in the single crystals with $x = 0.3$ is depressed smoothly, with a critical pressure $p_c \sim 6.3$ GPa where T_c vanishes [19]. Correspondingly, as shown in Fig. 2 the upper critical fields $B_{c2}{}^{ab}$ and $B_{c2}{}^{c}$ are suppressed with increasing pressure. At the highest achieved pressure of 2.31 GPa both ξ_{ab} and ξ_c have increased to 15 and 7 nm, respectively, but their ratio ξ_{ab}/ξ_c decreases to 2.1 from the value of 2.9 at $p = 0$. The gradual increment of the residual resistivity ρ_0 under pressure can be attributed to a decrement of n [19], which allows one to deduce $l > \xi$ in the entire experimental pressure range. Interestingly, all $B_{c2}(T)$ data presented in Fig. 2 collapse on a universal function $b^*(t) = (B_{c2}/T_c)/|dB_{c2}/dT|T_c$ (Fig. 4). Here t is the reduced temperature $t = T/T_c$. The function $b^*(t)$ deviates from the behavior for a standard weak-coupling s-wave superconductor. In addition to the mean free path larger than the SC coherence length mentioned above, the detailed analysis of B_{c2} provides evidence for odd-parity SC, namely the absence of Pauli limiting behavior, and the $B_{c2}(T)$ temperature-variation which resembles the one of a polar triplet state [19]. Therefore, Cu-doped Bi_2Se_3 is a candidate for topological superconductivity with time-reversal invariance, a full superconducting gap and an odd parity Cooper pair state at zero field $B = 0$. These features required for topological superconductivity seem to be robust under high pressures.

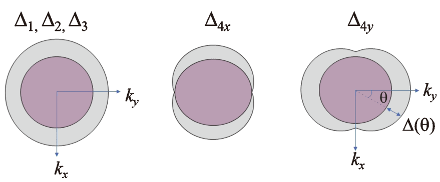

Fig. 3. (Color online) Cross-section views of Fermi surfaces and superconducting gaps in k_xk_y-plane (upper panel) for pairing potentials Δ_1, Δ_2, Δ_3 and Δ_4 (schematic) [8,26,28]. Note that Δ_{4x} and Δ_{4y} show point nodes in the y-direction and minima in the x-direction, respectively, which can be related to the RBS observed in doped Bi_2Se_3 superconductors.

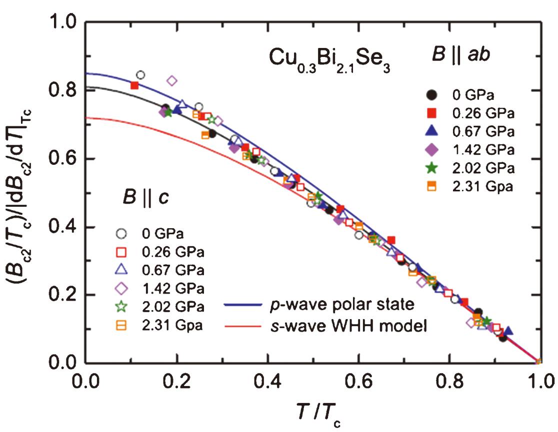

Fig. 4. (Color online) The upper critical filed B_{c2} normalized by the initial slope $|dB_{c2}/dT|T_c$ for $B//ab$-plane and $B//c$-axis as a function of the reduced temperature T/T_c for $Cu_{0.3}Bi_2Se_3$ [19].

4. Rotational symmetry breaking in Bi_2Se_3-based superconductors

The observation of rotational symmetry breaking in SC is a rare phenomenon and has recently been reported below the SC transition for the $M_xBi_2Se_3$ series of compounds with M = Cu [24,26], Sr [25] and Nb [27]. For instance, in the heavy fermion superconductor UPt_3 RSB has been reported under magnetic field in the C-phase [29]. Note that weak antiferromagnetic ordering detected in the normal state naturally breaks the rotational symmetry, but its effect on superconductivity is still controversial. In $Cu_xBi_2Se_3$ RSB is discovered in the superconducting state in the presence of time-reversal symmetry. As mentioned above, rhombohedral $Cu_xBi_2Se_3$, which is a bulk superconducting material with an optimum T_c of about 3.5 K, is a candidate for unconventional superconductivity. Strikingly, for $Cu_xBi_2Se_3$ with

$x = 0.3$ the two-fold in-plane field-angle dependences of the Knight shift measured at the ^{77}Se-nuclei [24] and the specific heat [26] provide solid evidence of RSB. The former leads also to a conclusion that the SC for M = Cu is of the spin-triplet type. The spin susceptibility (the Knight shift) should be small along the d-vector with minima at the x-direction for Δ_{4x}, as supported experimentally by field-angle dependent measurements of the specific heat [9,28]. From the latter it can be concluded that the SC gap for M = Cu is Δ_{4y}, possessing gap minima or nodes lying along the k_x-direction [9]. For these SC states the gap structures in momentum space are visualized in Fig. 3.

The RSB in Bi_2Se_3 based superconductors is not restricted to M = Cu. Actually, Sr-doped SC samples with various contents $x = 0.1$ and 0.15 exhibit a two-fold angular dependence of the upper critical field $B_{c2}(\theta)$ when the magnetic field is rotated in the aa^*-plane [25]. Hereafter, in order to visualize clearly a two-fold in-plane symmetry we use cartesian coordinates made by the a-, a^*- and c-axes. The a^*-axis is perpendicular to the a-axis and lies in the c-plane of the hexagonal coordinates of Bi_2Se_3. Consequently, "the aa^*-plane" is equivalent to the c-plane. As shown in Figs. 5a and 5b, the angular variations of B_{c2} for $x = 0.10$ and 0.15 determined by resistivity measurement under magnetic field exhibit a maximum at $B//a$-axis and a minimum at $B//a^*$-axis, and, consequently, a two-fold periodicity in the aa^*-plane. For M = Nb [27] the angular dependences of the effective spontaneous magnetization obtained from magnetic torque measurement below the SC transition breaks the rotational symmetry of the trigonal crystal, while above the SC transition the crystal symmetry is maintained to be three- or six-fold. According to a Ginzburg-Landau theory of B_{c2} in the D_{3d} crystal point group [30], a small in-plane anisotropy $\gamma^{aa^*} = B_{c2}{}^{a}/B_{c2}{}^{a^*} < 1$ and a six-fold periodicity in $B_{c2}(\theta)$ with respect to the azimuthal angle θ are realized. However, when a symmetry breaking term is introduced, for instance uniaxial strain in the trigonal basal plane, a two-fold in-plane symmetry in $B_{c2}(\theta)$ is derived, which leads the anisotropy of $\gamma^{aa^*} > 1$. γ^{aa^*} is theoretically displayed as a function of the uniaxial strain coupling g and the ratio J_4/J_1 of the gradient coefficients [30]. In the case of a uniaxial elastic interaction we expect to observe a crystal symmetry lowering from the trigonal crystal structure at least below T_c. It should be emphasized, however, that the symmetry breaking field required to establish the RSB has not been clarified unambiguously yet. Therefore, one of the important subjects related to the RSB seems to be pressure effects on the superconducting and crystallographic properties in the doped Bi_2Se_3 superconductors.

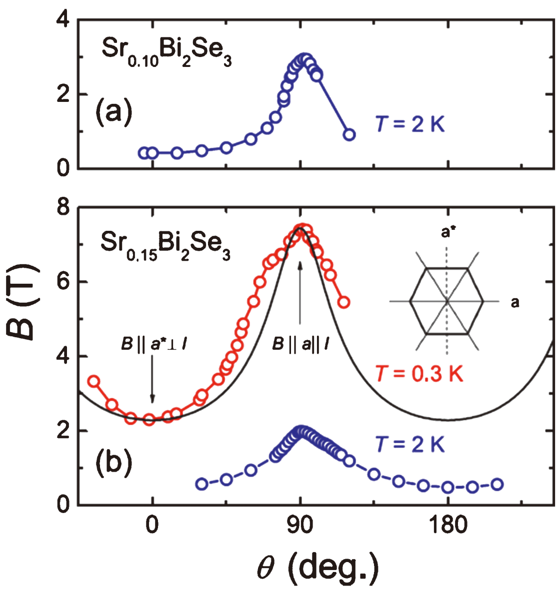

Fig. 5. (Color online) Angular variations of B_{c2} for $Sr_{0.10}Bi_2Se_3$ measured at $T = 2$ K (a) and for $Sr_{1.5}Bi_2Se_3$ at $T = 0.3$ and 2 K (b) under magnetic field directed in the trigonal basal plane [25].

5. Rotational symmetry breaking under high pressure

We would like to recall the characteristics of superconductivity in Sr-doped Bi_2Se_3 at ambient pressure. The SC properties for $x = 0.10$ and 0.15 are listed in Table 1 [25]. Examining the SC properties for these samples Pan *et al.* concluded: (i) both samples exhibit a two-fold anisotropy of the basal plane B_{c2} with $\gamma^{aa^*} = 6.8$ (at 1.9 K) and 3.2, respectively, (ii) the large γ^{aa^*} cannot be explained with the anisotropic effective mass model or the variation of B_{c2} caused by flux flow, (iii) unconventional superconductivity, with an odd-parity triplet paring state (Δ_4) is realized, or, otherwise superconducting stripes form due to preferential ordering of the dopant atoms.

Since in general the magnetic field in a cryostat is directed along the long direction of the piston-cylinder-type pressure cell it is not possible to make meaningful field-angle dependent measurements. Therefore, in order to investigate γ^{aa*} as a function of pressure two $Sr_xBi_2Se_3$ single crystals ($x = 0.15$) cut along the a- and a^*-axis were fixed on a sample stage for resistance measurement under high pressure [22] and aligned with the magnetic field direction in the pressure cell. Fig. 6 shows the temperature variation of B_{c2} defined as the midpoint of the resistance drop at the SC transition with the configuration $B//a$ (left panel) and $B//a^*$ (right panel) at various pressures. Note that the vertical scales of the left and right panels differ a factor of 2. Remarkably, T_c at zero field is depressed significantly and concomitantly, both $B_{c2}{}^a$ and $B_{c2}{}^{a*}$ are also suppressed with increasing pressure. The critical pressure is estimated to be $p_c = 3.5$ GPa by a linear extrapolation of $T_c(p)$. Note that the value of $B_{c2}{}^a$ at $T \to 0$ exceeds the Pauli limit $B^P = 1.86 \times T_c \sim 5.6$ T for a spin-singlet SC [25]. The anisotropy $\gamma^{aa*} = B_{c2}{}^a/B_{c2}{}^{a*}$ is enhanced under pressure and reaches a value of ~ 6 at 2 GPa, as shown in the inset of Fig. 6 (right panel) [22].

The RSB observed below the SC transition gives insight into the determination of the SC pairing symmetry of $M_xBi_2Se_3$, a candidate TSC. The high pressure investigation of the SC properties suggests a scaling of the anisotropy γ^{aa*} related to the driving force of the RSB. The scaling of γ^{aa*} with respect to $p_c - p$, the distance from the critical point where SC is suppressed to $T_c = 0$, is shown in Fig. 7 for the superconductors of M = Cu and Sr. Interestingly, it shows that γ^{aa*} is enhanced as pressure approaches p_c, as indicated by the dashed curve in Fig. 7. Note that the normal state loses its metallic character gradually [19,20,22] and the carrier number n decreases with increasing pressure [19]. One of the plausible scenarios to explain the enhancement of γ^{aa*} is the occurrence of a pressure-induced crystallographic instability associated with an ETT in the vicinity of p_c, and which is coupled to the SC order parameter and results in

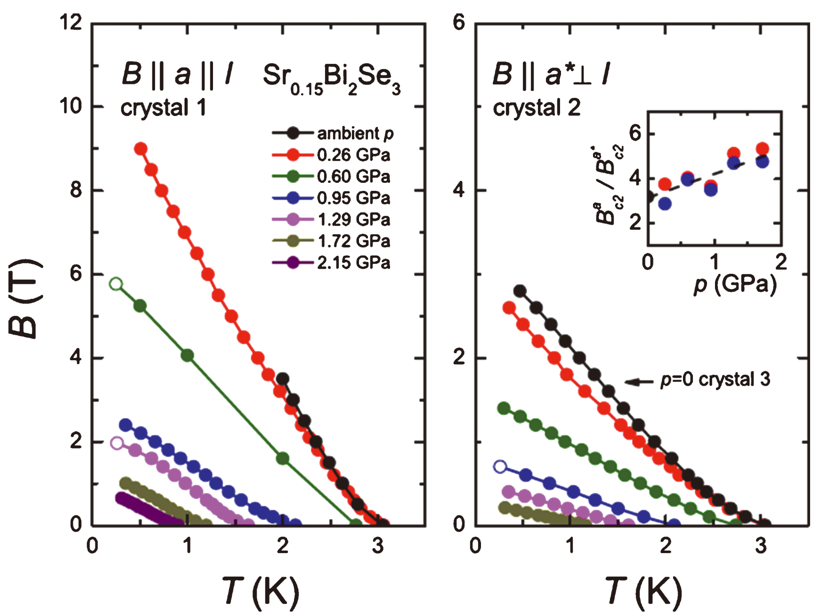

Fig. 6. (Color online) $B_{c2}(T)$ at various pressures determined by the resistivity measurements with the configurations of $B//a//I$ (left panel) and $B//a^* \perp I$ (right panel) for $Sr_{0.15}Bi_2Se_3$. Inset in the right panel shows $B_{c2}{}^a/ B_{c2}{}^{a*}$ ($= \gamma^{aa*}$) as a function of pressure [22].

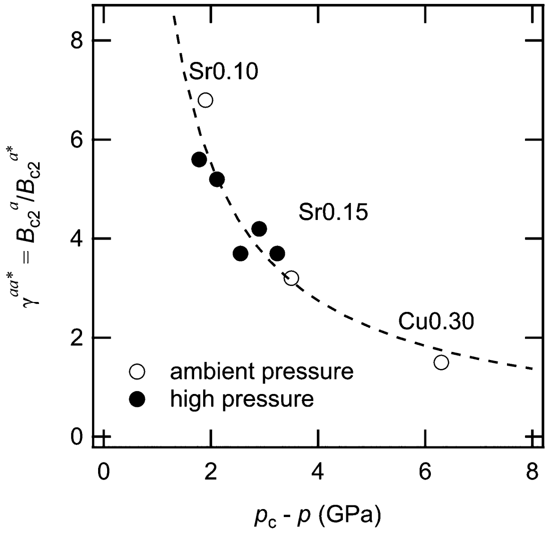

Fig. 7. The in-plane anisotropy of the upper critical field $\gamma^{aa*} = B_{c2}{}^{a}/B_{c2}{}^{a*}$ as a function of $p_c - p$.

the RSB below p_c. Assuming the symmetry breaking force to be uniaxial strain coupling and employing the Ginzburg Landau theory for B_{c2} [30], one can deduce that the coupling constant g and the ratio J_4/J_1 are strengthened under pressure in $M_xBi_2Se_3$. Actually, a low temperature limit of γ^{aa*} is given by $\sim (1+J_4/J_1)/(1-J_4/J_1)$, leading to a significant enhancement as the ratio approaches to $J_4/J_1 \sim 1$, while the coupling g shifts T_c. Microscopically, the origin of the symmetry breaking force is a Fermi surface distortion due to the uniaxial interaction, which couples to the SC order parameter, accelerates a shift of T_c and brings about the nematic ordering below T_c, that is, the nematic directors align parallel to one of the crystallographic axes in the trigonal basal plane [30]. Another scenario has been suggested in the recent literature [31]. Here it is claimed that a domain (ordered nematic domain) structure in the SC state can be controlled by applying a uniaxial strain along the aa^*-plane. Careful inspection of $B_{c2}(\theta)$ under uniaxial strain reveals that the in-plane angular dependence of B_{c2} is distorted from a simple two-fold symmetric one, which suggests that an examined single crystal consists of several nematic domains. Generally, a multi-domain structure consists of various nematic domains whose ordered nematic directors point along certain crystal axes in the basal plain with $\theta = \pm 2\pi/3$ and 0, respectively. Applying uniaxial strain along the a- or a^*-axis, a single nematic domain can be established. We cannot rule out the possibility that even under hydrostatic (homogeneous) pressure the multidomain structure is stimulated to transform to a single nematic domain structure, which results in an apparent enhancement of γ^{aa*} under pressure.

6. Summary

A review is presented of high pressure studies carried out on doped Bi_2Se_3 superconductors, in the context of their candidature for topological superconductivity. Focusing on the pressure range below the pressure-induced crystallographic transition, we argue the SC properties of $M_xBi_2Se_3$ for M = Cu, Sr and Nb are in line with an unconventional, time-reversal-invariant odd-parity spin-polarized state, as required for topological superconductivity. These are robust features under pressure. A striking ubiquitous element of the SC state in doped Bi_2Se_3 is rotational symmetry breaking (RSB) and which is enforced under high pressure. It is proposed that one of the characteristics of the RBS, the two-fold anisotropy of the upper critical field in the trigonal basal plane of $M_xBi_2Se_3$, diverges at $p \approx p_c$. The current data call for further high pressure studies that could provide insight not only in the SC gap symmetry of TSCs, but also in potential conventional and topological Lifshitz transitions in these fascinating materials.

Acknowledgment

This work was partially supported by a Grant-in-Aid for Scientific Research, KAKENHI, Grant Number 20H01851 and the JSPS (Japan Society for the Promotion of Science) Program for Fostering Globally Talented Researchers, Grant Number R2903.

Reference

[1] M. Kriener, K. Segawa, Z. Ren, S. Sasaki, Y. Ando: Phys. Rev. Lett., **106**, 127004 (2011).
[2] Y.S. Hor, A.J. Williams, J.G. Checkelsky, P.

Roushan, J. Seo, Q. Xu, H.W. Zandbergen, A. Yazdani, N.P. Ong, R.J. Cava: Phys. Rev. Lett., **104**, 057001 (2010).
[3] Z. Liu, X. Yao, J. Shao, M. Zuo, L. Pi, S. Tan, C. Zhang, Y. Zhang: J. Am. Chem. Soc., **137**, 10512 (2015).
[4] Y. Qiu, K.N. Sanders, J. Dai, J.E. Medvedeva, W. Wu, P. Ghaemi, T. Vojta, Y.S. Hor: arXiv:1512.03519.
[5] H. Zhang, C.-X. Liu, X.-L. Qi, X. Dai, Z. Fang, S.-C. Zhang: Nat. Phys., **5**, 438 (2009).
[6] L.A. Wray, S.Y. Xu, Y. Xia, Y.S. Hor, D. Qian, A.V. Fedorov, H. Lin, A. Bansil, R.J. Cava, M.Z. Hasan: Nat. Phys., **6**, 855 (2010).
[7] C.Q. Han, H. Li, W.J. Chen, F. Zhu, M.-Y. Yao, Z.J. Li, M. Wang, B.F. Gao, D.D. Guan, C. Liu, C.L. Gao, D. Qian, J.-F. Jia: Appl. Phys. Lett., **107**, 171602 (2015).
[8] L. Fu, E. Berg: Phys. Rev. Lett., **105**, 097001 (2010).
[9] S. Yonezawa: Condens. Matter, **4**, 2 (2019).
[10] R. Vilaplana, D.S. Pérez, O. Gomis, F.J. Manjoń, J. González, A. Segura, A. Muñoz, P.R. Hernández, E.P. González, V.M. Borrás, V.M. Sanjose, C. Drasar, V. Kucek: Phys. Rev. B, **84**, 184110 (2011).
[11] K. Kirshenbaum, P.S. Syers, A.P. Hope, N.P. Butch, J.R. Jeffries, S.T. Weir, J.J. Hamlin, M.B. Maple, Y.K. Vohra, J. Paglione: Phys. Rev. Lett., **111**, 087001 (2013).
[12] Z. Yu, L. Wang, Q. Hu, J. Zhao, S. Yan, K. Yang, S. Sinogeikin, G. Gu, H. Mao: Sci. Rep., **5**, 15939 (2015).
[13] A. Bera, K. Pal, D.V.S. Muthu, U.V. Waghmare, A.K. Sood: J. Phys.: Condens. Matter, **28**, 105401 (2016).
[14] A. Polian, M. Gauthier, S.M. Souza, D.M. Triches, J.C. Lima, T.A. Grandi: Phys. Rev. B, **83**, 113106 (2011).
[15] A. Nakayama, M. Einaga, Y. Tanabe, S. Nakano, F. Ishikawa, Y. Yamada: High Pressure Res., **29**, 245 (2009).
[16] A. Bera, K. Pal, D.V.S. Muthu, S. Sen, P. Guptasarma, U.V. Waghmare, A.K. Sood: Phys. Rev. Lett., **110**, 107401 (2013).
[17] I.M. Lifshitz: Sov. Phys. JETP, **11**, 1130 (1960).
[18] G.E. Volovik: arXiv:1606.08318v6.
[19] T.V. Bay, T. Naka, Y.K. Huang, H. Luigjes, M.S. Golden, A. Visser: Phys. Rev. Lett., **108**, 057001 (2012).
[20] Y. Zhou, X. Chen, R. Zhang, J. Shao, X. Wang, C. An, Y. Zhou, C. Park, W. Tong, L. Pi, Z. Yang, C. Zhang, Y. Zhang: Phys. Rev. B, **93**, 144514 (2016).
[21] K. Manikandan, Shruti, P. Neha, G.K. Selvan, B. Wang, Y. Uwatoko, K. Ishigaki, R. Jha, V.P.S. Awana, S. Arumugam, S. Patnaik: Europhys. Lett., **118**, 47008 (2017).
[22] A.M. Nikitin, Y. Pan, Y.K. Huang, T. Naka, A. Visser: Phys. Rev. B, **94**, 144516 (2016).
[23] M.P. Smylie, K. Willa, K. Ryan, H. Claus, W.-K. Kwok, Y. Qiu, Y.S. Hor, U. Welp: Physica C, **543**, 58 (2017).
[24] K. Matano, M. Kriener, K. Segawa, Y. Ando, G.-Q. Zheng: Nat. Phys., **12**, 852 (2016).
[25] Y. Pan, A.M. Nikitin, G.K. Araizi, Y.K. Huang, Y. Matsushita, T. Naka, A. Visser: Sci. Rep., **6**, 28632 (2016).
[26] S. Yonezawa, K. Tajiri, S. Nakata, Y. Nagai, Z. Wang, K. Segawa, Y. Ando, Y. Maeno: Nat. Phys., **13**, 123 (2017).
[27] T. Asaba, B. Lawson, C. Tinsman, L. Chen, P. Corbae, G. Li, Y. Qiu, Y. Hor, L. Fu, L. Li: Phys. Rev. X, **7**, 011009 (2017).
[28] L. Fu: Phys. Rev. B, **90**, 100509 (2014).
[29] Y. Machida, A. Itoh, Y. So, K. Izawa, Y. Haga, E. Yamamoto, N. Kimura, Y. Onuki, Y. Tsutsumi, K. Machida: Phys. Rev. Lett., **108**, 157002 (2012).
[30] J.W.F. Venderbos, V. Kozii, L. Fu: Phys. Rev. B, **94**, 094522 (2016).
[31] I. Kostylev, S. Yonezawa, Z. Wang, Y. Ando, Y. Maeno: Nat. Commun., **11**, 4152 (2020).

[Received July 30, 2020, Accepted October 8, 2020]